Heavy Ions Radiation Effects on 4kb Phase-Change Memory

Anna Lisa Serra, Tobias Vogel, Gauthier Lefevre, Stefan Petzold, Nico Kaiser, Guillaume Bourgeois, Marie-Claire Cyrille, Lambert Alff, Christina Trautmann, Christophe Vallée, et al.

▶ To cite this version:

Anna Lisa Serra, Tobias Vogel, Gauthier Lefevre, Stefan Petzold, Nico Kaiser, et al.. Heavy Ions Radiation Effects on 4kb Phase-Change Memory. NSREC 2020 - Nuclear and Space Radiation Effects Conference, Dec 2020, Virtual Event, United States. cea-03086369

HAL Id: cea-03086369

https://hal-cea.archives-ouvertes.fr/cea-03086369

Submitted on 22 Dec 2020

Phase-Change Memory

Based on ***Phase-Change Materials***:

<u>Ex</u>: $Ge_2Sb_2Te_5$ (GST), GeTe, etc.

- ***Amorphous*** phase (***logic state 0, RESET)***
- ***Crystalline*** phase (***logic state 1, SET)***

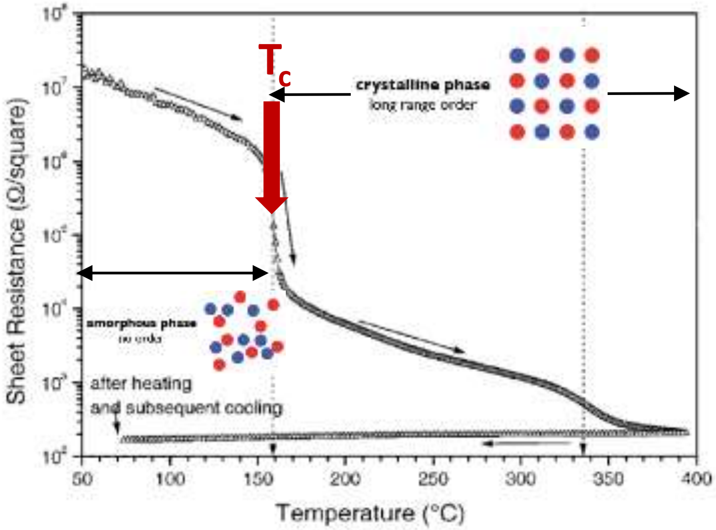

Fig.1 Resistivity as a function of temperature of a Phase-Change Material [1]

Memory programming relies on temperature profile control and <u>not on charge storage</u>

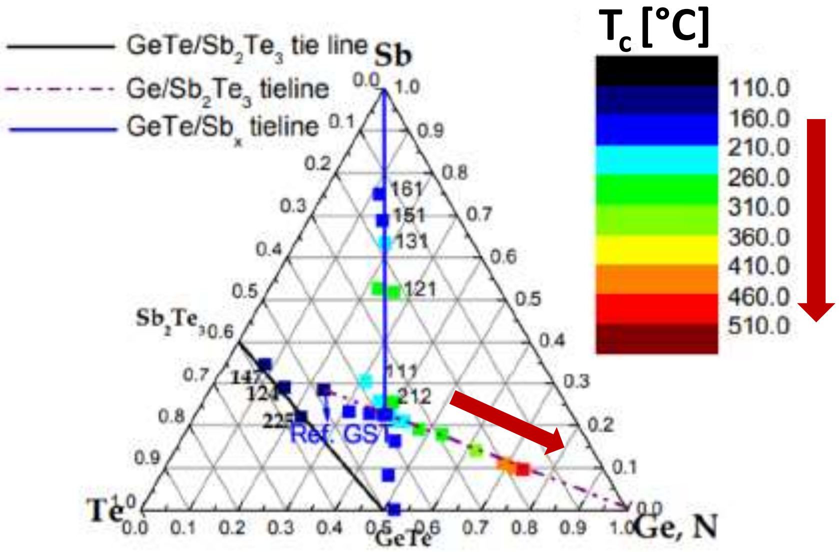

The crystallization temperature (T_c) can be tuned by engineering the material composition (Ge or N enrichment)

Fig.2 Crystallization temperatures T_c as a function of compositions in the Ge-Sb-Te ternary phase diagram [2]

[1] W. K. Njoroge, 2002
[2] H. Y. Cheng, 2012

PCM & radiation hardness

Radiation effects on the external circuitry

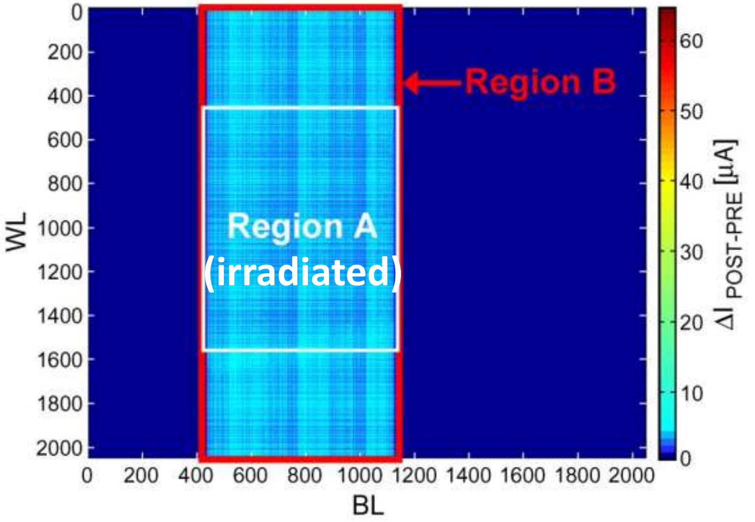

Fig. 3 Color map of the value of the cells of a MOS-chip array irradiated with a 30 Mrad SiO2 proton beam. Region A is the irradiated zone and Region B is the area were the cells show a change in current of more than 1 A with respect to the pre-irradiation condition [3].

Devices belonging to the same WL or BL are affected by radiation, even if they do not lie in the irradiated region

Radiation effects on scaled PCM

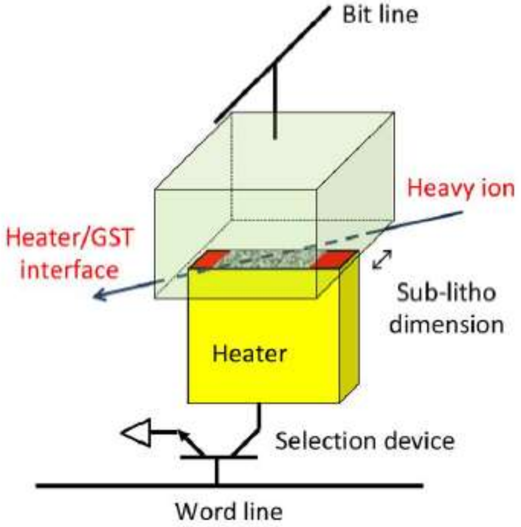

Fig. 4 Schematic of a phase change memory device hit by a heavy ion along the word line [4].

Partial amorphisation due to the temperature increase generated by the heavy-ions impinging on the active layer of 45 nm PCM

Radiation effect could impact the PCM depending on its device structure

[3] A. Gasperin, 2008, [4] S . Gerardin, 2014

Radiation effect on chalcogenide materials

GST and Ge-rich GeSbTe (GGST)

1. As deposited (amorphous)
2. Annealed at 450°C (polycrystalline)

Radiation effect on 4kb matrices

SET and RESET distribution

1. GST vs Ge-rich GeSbTe (w=100nm)
2. GST vs Interfacial Layer-PCM (w=300nm)

Irradiation beam specifications

- 8.3 MeV/u Au^{26+}-ions (E=1.635 GeV)
- Flux: 5E8 ions/cm^2 sec

- Fluences:
  10E9, 5E10, 10E12, 5E12, 7E12, 1E13 ions/cm^2

- Fluences :
  10E9, 5E10, 10E12 ions/cm^2

GST vs GGST

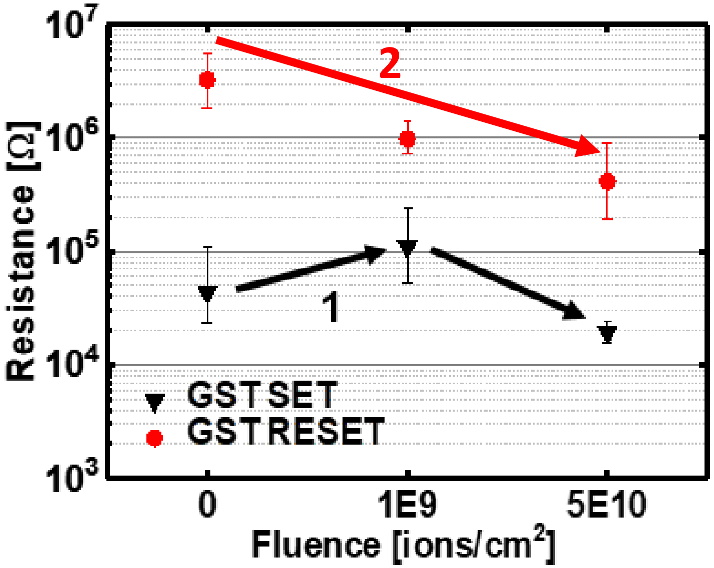

Fig. 5 Median and ±σ for SET and RESET distributions in GST 4kb arrays before and after irradiations at increasing fluences.

1. The SET state in GST faces a **structural relaxation** at a fluence of 10E9 ions/cm^2 plus amorphisation at 5e10 ions/cm^2
2. The GST RESET resistance decreases with increasing fluence

1.

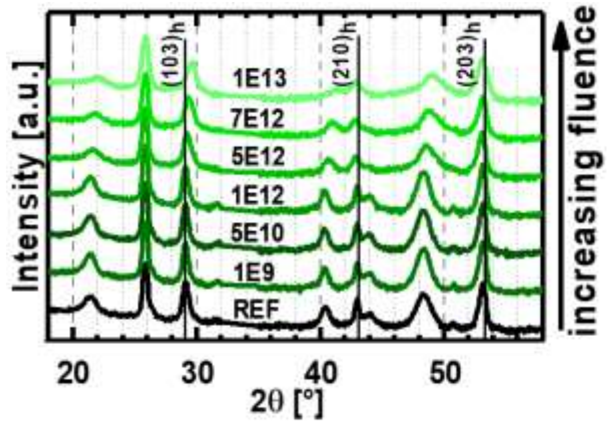

Fig. 6 XRD patterns of GST crystalline layers before (REF) and after irradiations at increasing fluence.

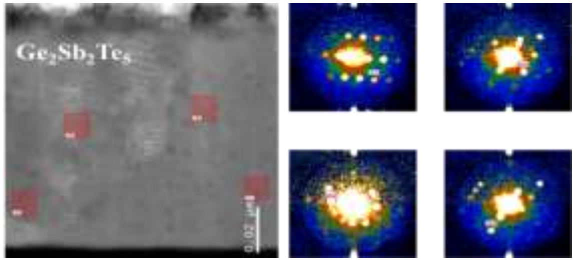

Fig. 7 TEM (left) and nano-diffraction patterns (right) analyses of as-deposited amorphous GST after irradiation at a fluence of 10^{13} ions/cm^2.

2.

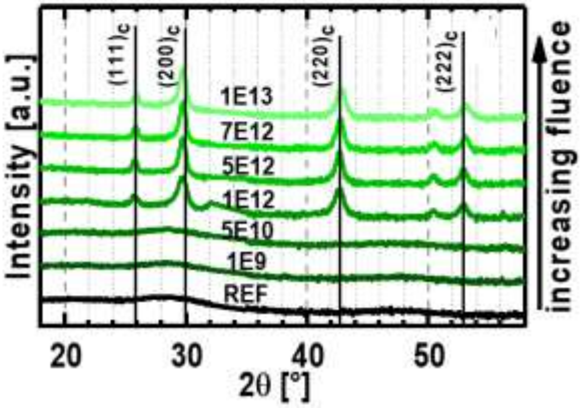

Fig. 8 XRD patterns of GST amorphous layers before (REF) and after irradiations at increasing fluence.

GST vs GGST

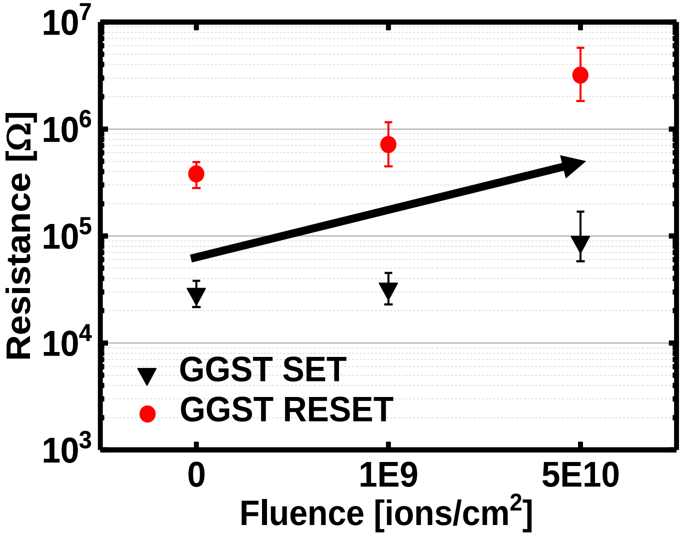

Fig. 9 Median and ±σ for SET and RESET distributions in GGST 4kb arrays before and after irradiations at increasing fluences.

SET and RESET states in GGST show structural relaxation at both fluences

Both the resistance window and the amorphous phase in the RESET state are preserved making GGST more stable than GST based devices thanks to its higher T_c

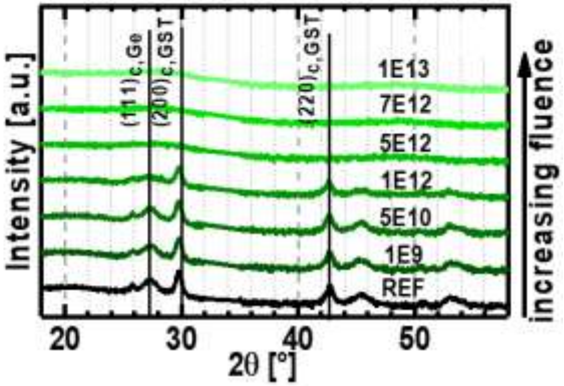

Fig 10 XRD patterns of GGST crystalline layers before (REF) and after irradiations at increasing fluence.

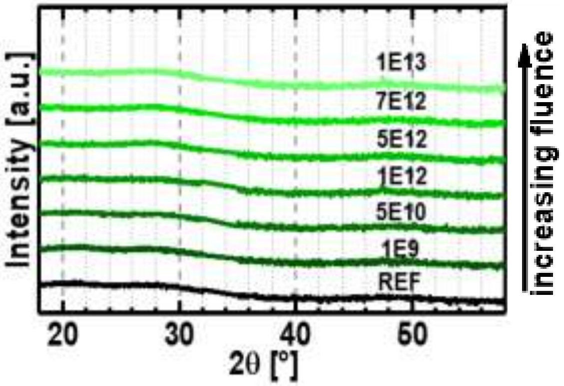

Fig 11 XRD patterns of GGST amorphous layers before (REF) and after irradiations at increasing fluence.

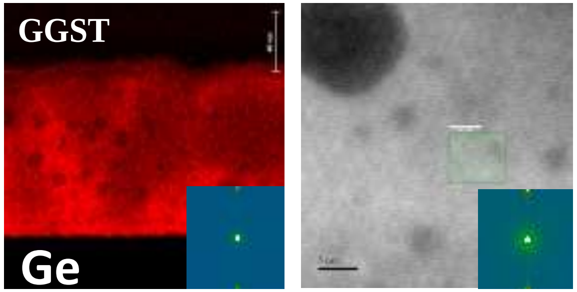

Fig 12 TEM/EDX and nano-diffraction patterns analyses of crystalline GGST after irradiation at a fluence of 7 × 10^{12} ions/cm^2. The Ge cartography (left) shows that the Ge segregation induced by the annealing process remains unchanged after irradiation. However, the irradiation reduces the size of the crystallites as evidenced by few and low intensity nano-diffraction patterns identified (right).

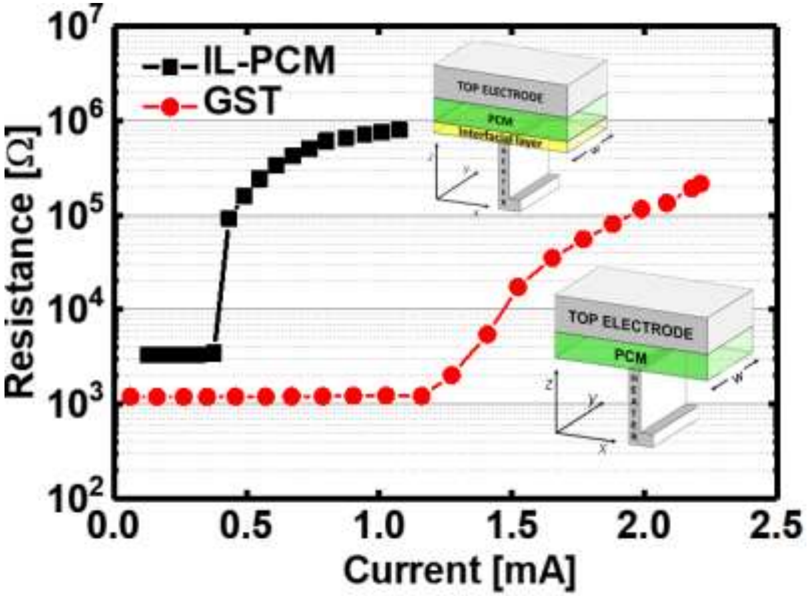

Fig. 13 Resistance-vs-Current characteristics comparing a standard GST device with an IL-PCM. IL-PCM shows a high current reduction wrt GST in devices featuring same critical dimension (electrode area $\sim 3 \times 10^{-3}$ µm^2).

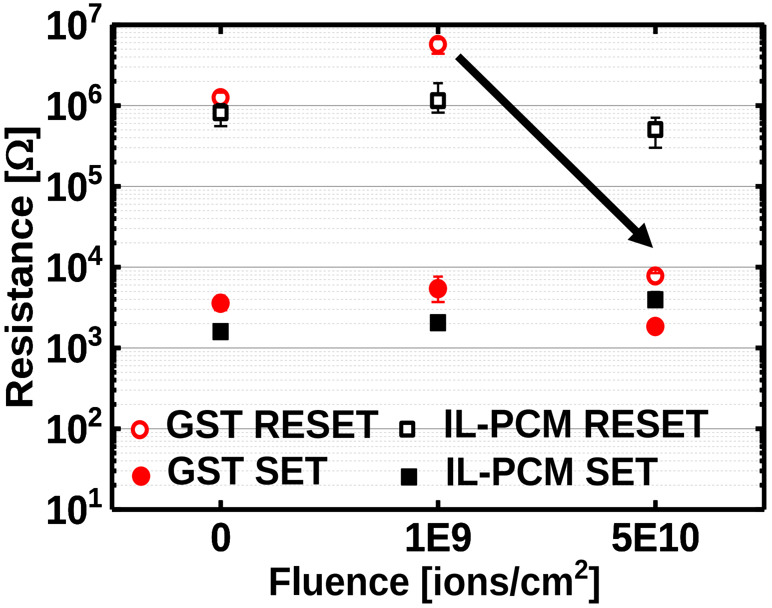

Fig. 14 Median and ±σ for SET and RESET distributions in GST and IL-PCM 4kb arrays before and after irradiations at increasing fluences.

GST vs IL-PCM

- Strong reduction in RESET current for IL-PCM wrt GST
- The higher SET resistance in IL-PCM is an evidence of the smaller contact area created during the programmig of the cell

IL-PCM shows a higher radiation tolerance due to the « smaller » contact area between heater and PCM

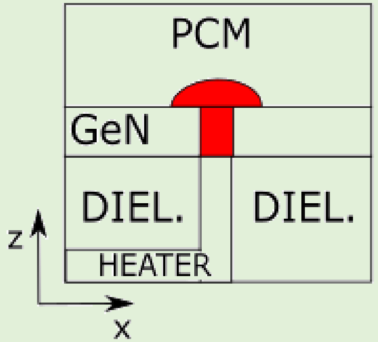

Fig. 15 Schematic of the zx-plane of an IL-PCM showing in red the programmed region, demonstrating the contact area reduction.